



OPEN Study on the in-situ modified support method of roadway surrounding rock under vertical impact load

Heng Zhang^{1✉}, Su Liu², HaiYang Yi³, Juntong Liu¹, Yan Qin¹, Yuqian Li¹, Yan Dong¹, Yong Cao⁴, Fangchao Lu^{5,6}, Shaoshuai Guo⁷, Tie Li^{8✉} & Yan Liu^{1✉}

With the deepening of coal mining, the frequency and intensity of rock burst accidents are increasing. According to incomplete statistics, there have been over 200 rock burst accidents in tunnels in China alone from 2005 to 2024, resulting in more than 500 deaths and causing extensive damage to tunnel equipment. Therefore, research on tunnel surrounding rock support methods is urgently needed. Based on a large number of previous studies on the surrounding rock support methods and technologies of coal mine roadway, this paper innovatively proposed the in-situ modified support method of roadway surrounding rock, and compared and analyzed the differences between the original rock roadway and the in-situ modified roadway surrounding rock in terms of static stress redistribution, displacement, plastic zone, dynamic stress and kinetic energy dissipation by using numerical simulation and laboratory experiments. The results show that the surrounding rock in the cracked region and reinforced region can redistribute the static stress of the roadway, better transfer the high static stress concentration distribution zone to the outside of the surrounding rock in the cracked region, and the dynamic stress transmitted to the surrounding rock surface of the roadway is reduced by about 1.29 ~ 4.0 times. Under the action of large vertical dynamic load, the displacement of surrounding rock in the roadway reinforcement area is reduced by about 1.9 ~ 4.0 times, the dynamic stress is reduced by about 37%~48%, and the overall plastic zone is significantly reduced. The plastic failure of coal and rock in the cracked region consumes and weakens the impact energy, enhances the dissipation effect of kinetic energy in surrounding rock, and effectively ensures the integrity of coal and rock in the reinforced region. The above research results can provide new support theory and technical ideas for surrounding rock support of roadways prone to rock bursts, prevent roadway rock burst accidents, and ensure mine safety production.

Keywords Rock burst, Roadway surrounding rock, In-situ modification, Static stress transfer, Dynamic stress transfer, Kinetic energy dissipation

With the depletion of shallow coal resources, coal mining is gradually shifting towards the deeper parts of the Earth^{1–3}. Coal rock formations located deep in the geological strata are often influenced by factors such as high ground stress and complex geological structures. When subjected to artificial mining and other geological activities, there is a severe impact damage phenomenon, which can easily lead to coal mine rock burst accidents, resulting in destructive consequences such as fully mechanized mining faces or roadway walls, floor bulges, roof falls, support failures, roadway blockages, equipment damage, and personnel injuries^{4–7}. Coal mine rock burst refers to the dynamic phenomenon of sudden and severe damage to the coal (rock) surrounding the coal mine

¹Occupational Hazards Control Technology Center, Beijing Academy of Science and Technology Institute of Urban Safety and Environmental Science, Beijing, China. ²School of Resources and Civil Engineering, Northeastern University, Shenyang, China. ³School of Safety Regulation, North China Institute of Science and Technology, Hebei, China. ⁴School of Mining Engineering, Anhui University of Science and Technology, Huainan 232001, China. ⁵College of Municipal and Environmental Engineering, Henan University of Urban Construction, Pingdingshan 467036, Henan, China. ⁶Pingdingshan Tian'an Coal Mining Co., Ltd, Pingdingshan 467036, Henan, China. ⁷School of Environmental and Municipal Engineering, North China University of Water Resources and Electric Power, Zhengzhou 450045, China. ⁸School of Civil and Resource Engineering, University of Science and Technology Beijing, Beijing, China. ✉email: zhanghengbk@163.com; liutie@ustb.edu.cn; liuyandhn@163.com

roadway or working face due to the instantaneous release of elastic deformation energy, often accompanied by instantaneous displacement, ejection, loud noise, and air waves of the coal (rock). Rock burst accidents seriously affect the safety production of mines, and most of them occur in tunnels. Therefore, tunnel support is a major problem to be solved in the coal mining process^{8–11}. For example, on February 22, 2020, a roadway rock burst occurred at Longgu Coal Mine of Shandong New Julong Energy Co., Ltd., resulting in 4 deaths and direct economic losses of 18.53 million yuan; On October 20, 2021, a roadway rock burst accident occurred in the second well of Lushan High Quality Coal Co., Ltd. in Qitaihe City, resulting in 3 deaths and direct economic losses of 3.27 million yuan. Most of the above rockburst accidents occur because the existing roadway support strength is not enough. Under the action of strong impact dynamic load, the supporting facilities such as supporting anchor cable net and supporting steel beam are greatly damaged, and the roadway is greatly deformed. The specific damage situation is shown in Fig. 1. When rockburst occurs, the roadway support and roadway surrounding rock are greatly damaged. Therefore, with the increase of coal mining depth, the supporting problem of impact roadway has become an urgent problem to be solved.

Aiming at the problem of roadway support, many scholars have studied support methods such as bolt, support and drilling pressure relief. Kanghongpu^{12–16} and others developed CRMG 700 high strength and high toughness anchor rod. It is pointed out that cable supports and roadway bolts, when enhanced by high-toughness bolts, can significantly improve the stability of the surrounding rock. Through the study of negative Poisson's ratio material, He et al.^{17–19} pointed out that it has large deformation's characteristics, and on this basis, a new type of anchor cable with negative Poisson's ratio material is studied, which has the characteristics of high deformability and constant resistance. It is pointed out that the constant resistance large deformation anchor cable can better accommodate slip deformation, thus absorbing the large energy produced by rock burst. The cable has a very good anti-scour support effect. Qi et al.^{20,21} proposed the anti-scour technology of "weak chain increasing consumption". By means of roof deep-hole blasting and floor presplitting, the stress in the dangerous area is reduced to ensure the integrity of the roadway and control the occurrence of rock bursts. Pan et al.^{22,23} studied roadway energy absorption and anti-impact support technology and suggested that when rock bursts occur, the damaging components can deform and absorb energy at the same time to protect the surrounding rock support equipment of the roadway. This ensures that roadway support facilities can protect against large impact kinetic energy and prevent the occurrence of rock bursts. Lu et al.^{24,25} proposed the use of steel plate support. The research results show that the force of the impact stress wave on the steel plate support is 30.7% less than that on the steel frame support, and the steel plate impact structure can absorb more than 90% of the impact energy. Huang et al.²⁶ studied the damper at the end of the anchor cable and found that increasing the supporting viscosity of the damper at the tail end can transform the mechanical energy of roadway rock burst into thermal energy, thus eliminating the degree of impact damage to the roadway. On this basis, a new type of anti-impact constant resistance anchor cable is studied. According to the research of Jiao et al.²⁷, it is pointed out that through the pressure relief of large diameter drilling in the deep, the superstrength bolt support in the shallow part, and the auxiliary support of metal retractable support on the roadway surface, the forces of roadway and bolt are in the controllable range when the impact occurs and the supporting effect is good. Anders Ansel^{28,29} developed an energy-absorbing anchor that can reduce deformation and yield with the movement of roadway surrounding rock. Gaudreau et al.³⁰ studied and analyzed the conical anchor; so they developed a bolt made of polyamine resin and added blades to it. The supporting bolt is verified by field experiments in several rock burst mines in Canada. When a rock burst occurs, the roadway supporting facilities are not obviously damaged, and the roadway remains relatively intact. Through the study of bolt material, D Raju Guntumadugu³¹ proposed that the strength and deformation of bolt material can be changed to absorb the energy caused by different impact expansions of rock. As a result, it has developed a new type of anchor. Li C C et al.^{32,33} suggested that the bolt can not only have two anchoring points but also have a certain supporting effect when the bolt has

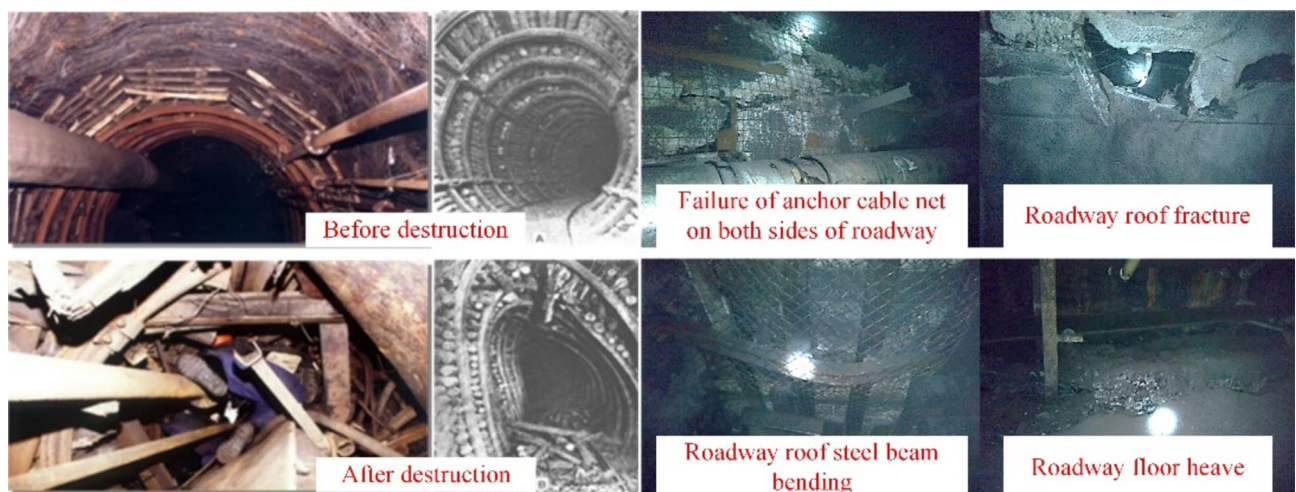


Fig. 1. Roadway rockburst failure diagram.

multiple anchoring points and some parts of the bolt are broken. As a result, D anchors with multiple anchoring points have been developed.

Although the techniques and above coal mine roadway anti-impact support methods have played a good guiding role in solving rock burst roadway support's problem and have been verified by a large number of engineering examples, in recent years, there are still many coal mine rock burst accidents in places such as the Longxing Coal Mine³⁴, Qianqiu Coal Mine³⁵, Yuejin Coal Mine³⁶, Tangshan Coal Mine³⁷ and so on. At present, the protection and treatment of rock bursts in coal mine roadways is still insufficient^{38–40}. Therefore, in order to effectively prevent casualties and equipment damage caused by rock burst in coal mine roadway, it is necessary to update the existing rock burst roadway support concept. Based on the design principle of rock burst support system proposed by Kaiser and Cai [41], this paper proposes a new method of roadway in-situ modified support, which changes passive support to active support, that is, by changing the physical and mechanical properties of roadway surrounding rock, forming cracked region and reinforced region, so as to transfer the peak stress to the depth of coal and rock mass, weaken the propagation of dynamic wave, dissipate kinetic energy and strengthen the bearing capacity of roadway. Gao et al.^{42,43} and Wang et al.⁴⁴ have also studied similar road anti scour support structures, but their roadway support uses measures such as external support materials and artificial shock absorption and isolation belts. Therefore, the in-situ modified support method of roadway surrounding rock proposed in this paper is scientific and feasible, and is worthy of further research and analysis. In this paper, through the establishment of full-scale numerical model and reduced size similarity simulation experiment system, the characteristics of stress, displacement, plastic zone, dynamic stress and kinetic energy dissipation of roadway surrounding rock under in-situ modified support method and unmodified state of roadway surrounding rock are studied, which provides a certain theoretical basis for the application of support method in practical engineering.

Basic conception of the in-situ modified support method for roadway surrounding rock

After coal mining, the roadway is often supported externally by O-shaped sheds to protect the surrounding rock of the roadway, which is equivalent to supporting the surrounding rock of the roadway with the same thickness^{45,46}. A mechanical model of the surrounding rock of the roadway under vertical impact dynamic load is established as shown in Fig. 2, with the radius of the roadway being a_1 and the thickness of the supporting surrounding rock being $a_2 - a_1$. From Fig. 1, it can be seen that the surrounding rock of the roadway is subjected to vertical impact dynamic loads. Although the supporting rock provides good support for the roadway, it also experiences high dynamic stress at this location, making it highly susceptible to roadway impact ground pressure.

Based on a large amount of previous research, this article proposes a method for transforming the passive support of roadway surrounding rock into active support. The preliminary idea is shown in Fig. 3, which illustrates the in-situ modified support method for roadway surrounding rock. The surrounding rock of the tunnel under high stress in the deep part is sequentially modified into a grouting reinforced region and a fragmentation cracked region, that is, blasting or hydraulic fracturing is carried out on the coal rock mass in the deep part of the borehole (far away from the tunnel) to increase its damage degree, and grouting and other reinforced technology measures are taken on the coal rock mass in the shallow part (near the tunnel) to increase its integrity. An innovative in-situ modification support method for rock mass of the impact ground pressure mine tunnel is proposed.

Specifically, it refers to the process of crushing the surrounding coal and rock mass when the impact dynamic load propagates towards the center of the roadway, setting up a cracked coal and rock mass zone to form a circular cracked region, absorbing and dissipating the kinetic energy transmitted by the vibration wave, constructing an energy absorbing buffer structure, and reducing the propagation of dynamic load to the dynamic stress wave of the roadway. At the same time, the fragmentation of the surrounding rock in the tunnel leads to the transfer of high stress concentration areas to the outside of the cracked region, reducing the supporting pressure on the surrounding rock in the tunnel. Reinforce the coal rock mass around the tunnel to form a circular reinforced region, increasing its ultimate bearing strength. The reinforced region has strong bearing capacity, increasing its ability to store ultimate elastic-plastic deformation energy and elastic strain energy, and can bear the large kinetic energy brought by impact dynamic loads. It effectively resists the influence of dynamic stress propagation and static stress of overlying rock layers, improves the stability of the tunnel surrounding rock itself, and prevents the occurrence of tunnel impact ground pressure accidents. By transforming the surrounding rock of the roadway to fully absorb and dissipate kinetic energy, optimizing the stress state of the roadway, a in-situ modified support method for roadway surrounding rock is formed.

General situation of the project

Taking the first working face of a mine in Xinjiang as the engineering background, this paper studies the in-situ modified support method of roadway surrounding rock. This working face's main coal seam is the B₂ coal seam, and the working face's buried depth is approximately 400 m. The working face's inclination length is 152 m, the mining strike length is 1469 m, the mining height is 3.2 m, the coal that draws thickness is 6.3 m, and the working face's average inclination angle is 14°. Within 100 m of the overlying roof, there is mostly sandstone, and there are many thick and hard strata. The specific top and bottom strata of B₂ coal seam are shown in Table 1. The roadway of this working face is supported by an O-shaped shed. The B₂ coal seam and floor strata have a weak impact tendency, and the roof strata have a strong impact tendency. Three large energy events of more than 5 power were detected in the mine, which were about 3.1×10^6 J, 9.7×10^6 J and 9.1×10^6 J, respectively, resulting in different degrees of roadway side and roof subsidence, one anchor beam was broken, four anchor cables were broken, and three single hydraulic props were pushed down. The rock burst is mainly caused by the pressure

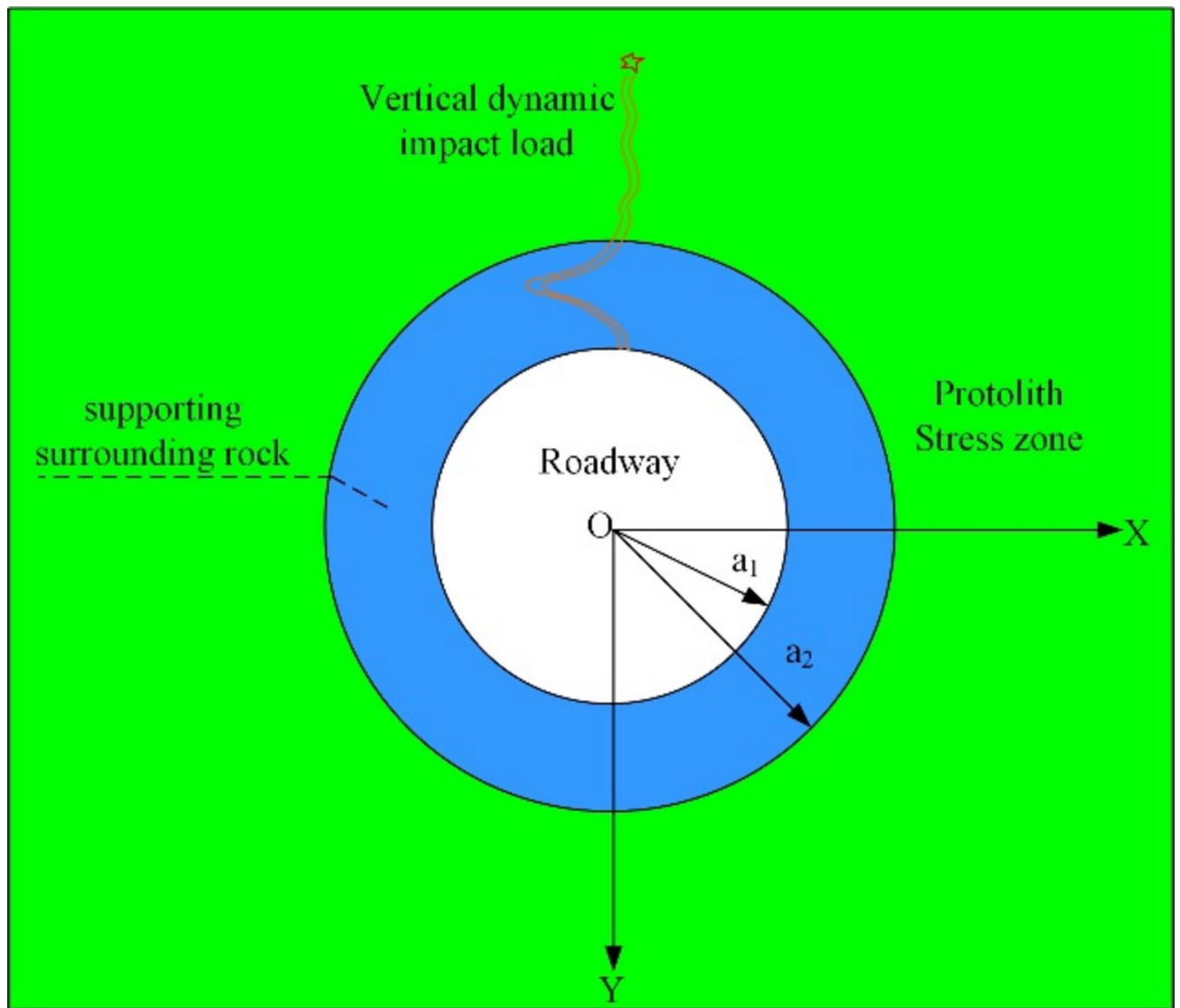


Fig. 2. Model of mechanical action of vertical impact dynamic load on roadway surrounding rock.

above the roadway roof, which causes the roadway surrounding rock to be subjected to large impact dynamic load. When a large energy event occurs in the roadway roof, the existing roadway support measures in the working face cannot absorb the impact energy instantly, and the roadway support equipment and surrounding rock are prone to deformation and damage. The roadway support measures cannot meet the requirements of impact protection, and it is extremely difficult to prevent the occurrence of rock burst.

Methods

Based on the real overview of each rock layer in the working face mentioned above, this paper establishes physical similarity models and numerical models.

Similar model design and experimental scheme

In the similarity simulation experiment, three kinds of similarity are mainly considered: geometric similarity, kinematic similarity and dynamic similarity. In the similarity theory, if two objects are geometrically, dynamically and kinematically similar, it is considered that the physical phenomena of the two objects are similar. In the dynamics problem, the geometric similarity is easy to achieve, but the dynamics similarity experiment is difficult, and it is the key point of the similarity simulation experiment.

Under static conditions, the stress relationship between roadway support and surrounding rock can be expressed as:

$$\sigma = f(F, \rho, g, \mu, l, c, \phi, E, t) \quad (1)$$

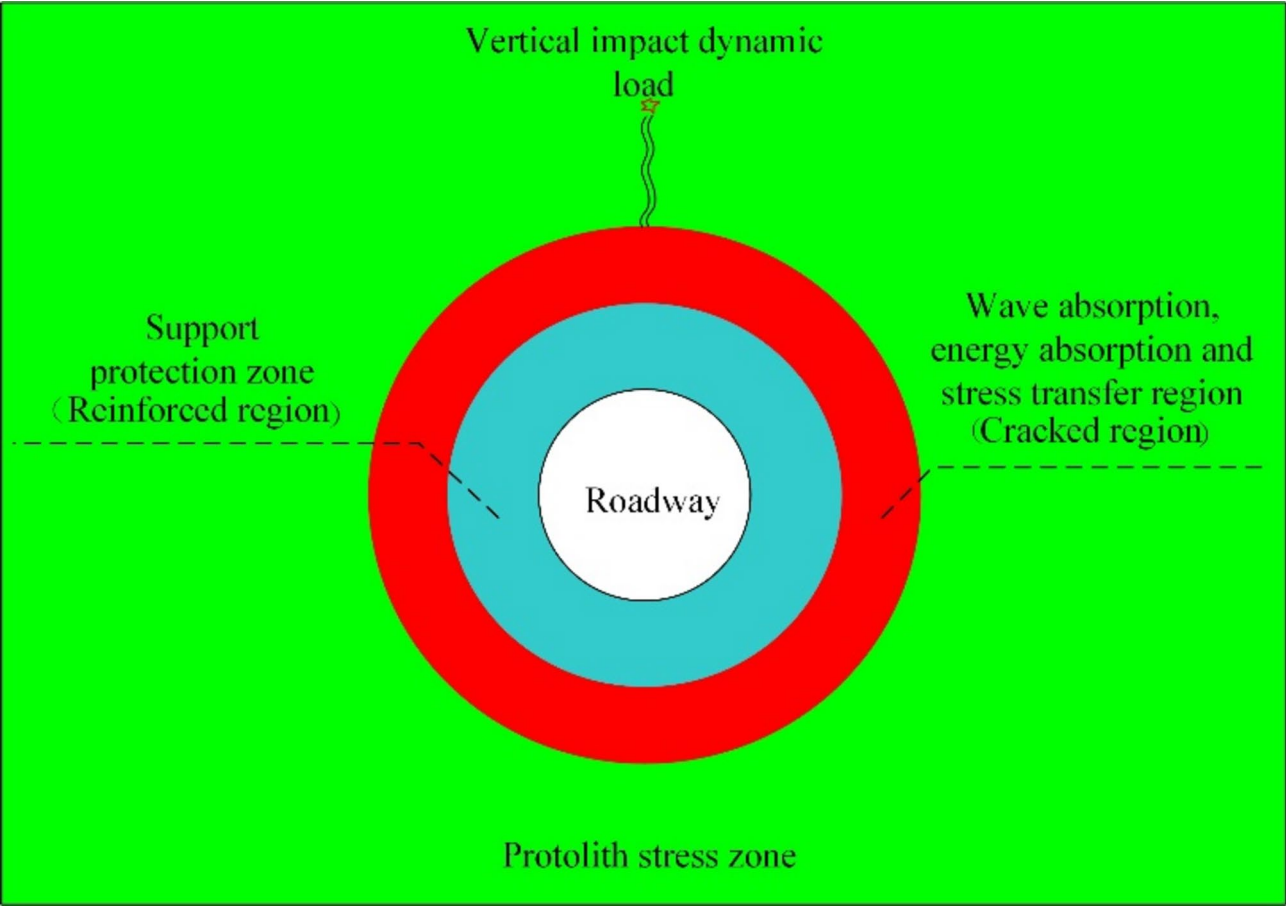


Fig. 3. Schematic diagram of in-situ modified support method for roadway surrounding rock.

Serial number	Lithology	Lithology	Thickness/m
1		Fine sandstone	26.0
2		Sandy mudstone	6.0
3		Coarse sandstone	7.6
4		B ₄ ² coal seam	1.5
5		Fine sandstone	9.6
6		B ₄ ¹ coal seam	4.0
7		Fine sandstone	9.0
8		Coarse sandstone	8.0
9		B ₃ coal seam	1.8
10		Siltstone	4.8
11		Fine sandstone	19.3
12		B ₂ coal seam	11.8
13		Sandy mudstone	4.0
14		Coarse sandstone	22.0
15		B ₁ coal seam	7.0
16		Sandy mudstone	15.0

Table 1. Top and bottom strata of B₂ coal seam.

In the above formula: $l, \rho, e, G, \sigma, C, \phi, \mu, F, \epsilon, t$ represent length, density, elastic modulus, gravitational acceleration, stress, cohesion, internal friction angle, strain, force, energy and time respectively.

The dynamic characteristics of elastic continuum can be expressed by the following equation:

$$[M] \{a\} + [C] \{v\} + [K] \{u\} = \{R\} \tag{2}$$

Where: m is the quality matrix; A is the acceleration matrix; C is the damping matrix; V is the velocity matrix; K is the static stiffness matrix; U is the displacement matrix; R is the load matrix.

According to the similarity simulation theorem and the dimensionless analysis method, the length L , density ρ and elastic modulus E are determined as the basic dimensional criteria. The similarity relationship is deduced according to the similarity law, and the following similarity criteria are obtained:

$$\begin{cases} C_{\sigma} = C_E = C_c \\ C_F = C_E C_l^2 \\ C_g = C_E C_{\rho}^{-1} C_l^{-1} = 1 \\ C_{\mu} = C_{\phi} = 1 \end{cases} \tag{3}$$

$$\begin{cases} C_u = C_l \\ C_a = C_g = C_E C_{\rho}^{-1} C_l^{-1} \\ C_v = C_{\rho}^{-0.5} C_E^2 \\ C_t = C_{\rho}^{0.5} C_E^{-0.5} C_l^1 \end{cases} \tag{4}$$

According to the similarity law, the geometric similarity ratio is 1:100, and the density similarity ratio is 1:1.5. Because both the similarity model and the actual situation are in the same gravity field, the acceleration ratio is 1:1. The full similarity of the controlled physical and mechanical parameters is realized in the elastic range, and the similarity ratio between the prototype value and the model value of each physical parameter is deduced according to the similarity criterion, as shown in Table 2. In the table, $l, \rho, E, t, u, g, \sigma, c, \phi, \epsilon, \mu, V, a, F$, and e represent length, density, elastic modulus, time, displacement, gravity acceleration, stress, cohesion, internal friction angle, strain, Poisson's ratio, velocity, acceleration, force and energy, respectively, and the symbol C represents similarity.

According to the previous experience of similar simulation experiments, sand, lime and gypsum are selected as similar model materials in this experiment. In the reinforced region, the elastic modulus is increased by reducing the content of sand and increasing the content of gypsum and diatomite (approximately 10% of the unmodified surrounding rock). The cracked region increases the sand content and adds a large number of mica sheets to increase its fissures to reduce its elastic modulus (approximately 90% of the unmodified surrounding rock). By preparing standard samples for uniaxial compression testing of elastic modulus under different ratios, the material ratios of each rock layer, reinforced region, cracked region, and supporting rock zone that meet the similarity ratio of elastic modulus are analyzed. Uniaxial compression tests were conducted on samples of sand gypsum, sand gypsum diatomaceous earth, and sand gypsum mica flakes with different ratios, as shown in Fig. 4. Based on the results of uniaxial compression testing and the determined similarity ratio of elastic modulus 1:150, the material ratio of each rock layer in the similar model was finally determined. The water consumption for each layer is about 1/10 of the total weight of the material, as shown in Table 3.

The physical similarity model is shown in Fig. 5. The model is laid layer by layer, and each layer is compacted with a heavy hammer, as shown in Fig. 5a. For the reliability of the experimental results, black plastic foam is pasted around the model to absorb energy to eliminate the effect of dynamic wave rebound, as shown in Fig. 5b. The unmodified roadway is supported by a PVC plastic pipe, and an equivalent surrounding rock support region with a thickness of 10 mm is processed on the outside of the plastic pipe to simulate the O-shaped shed support of the roadway. The PVC pipe is drawn out after completion. For the surrounding rock of the in-situ modified roadway, the cracked region is filled with aluminum skin in advance and placed in the corresponding position of the rock stratum. To achieve the purpose that the cracked region is not loaded, the aluminum shell is removed, and then the reinforced region is filled, as shown in Fig. 5c. According to previous research experience and comprehensive consideration of the field working conditions of the abovementioned working face, the roadway's diameter is 40 mm, the reinforced region's ring diameter is 40 mm, and the cracked region's ring diameter is 50 mm. According to the data of the coal strata in Table 1, there are 14 layers in the model. The rock strata within 100 m above the roadway and 30 m below the floor are simulated, with an unmodified roadway on the left and

Physical quantity	Symbols and relations	Similarity coefficient	Physical quantity	Symbols and relations	Similarity coefficient
Length	C_l	100	Internal friction angle	$C_{\phi} = 1$	1
Density	C_{ρ}	1.5	Strain	$C_{\epsilon} = 1$	1
Elastic modulus	$C_E = C_{\rho} C_g C_l$	150	Poisson's ratio	$C_{\mu} = 1$	1
Time	$C_t = C_l^{0.5}$	10	Speed	$C_v = C_E^{0.5} C_{\rho}^{-0.5}$	10
Displacement	$C_u = C_l$	100	Acceleration	$C_a = C_g$	1
Stress	$C_{\sigma} = C_E$	150	Force	$C_F = C_{\rho} C_g C_l^3$	1.5×10^6
Cohesive force	$C_c = C_E$	150	Energy	$C_e = C_F C_l$	1.5×10^8

Table 2. Similarity coefficient table of physical quantities in similarity model experiment.



Fig. 4. Uniaxial compression test.

an in-situ modified roadway on the right. The roof of the roadway is 1 m away from the upper surface, and the distance between the two roadways is 1 m. Finally, a physical model with a length of 2 m, a height of 1.3 m and an inclination of 14° is formed, as shown in Fig. 5e. After all the model layers are completed, the iron block with a height of approximately 0.28 m and total pressure of 21.5 kPa is used to model the overburden weight (approximately 300 m overburden weight), as shown in Fig. 5d. The pressure sensors provided by the Institute of Engineering Mechanics of the China Seismological Bureau are buried in the model. The landfill positions of the pressure sensors are as follows: M1 and M2 at the center and outside 50 mm of the equivalent surrounding

Lithology	Thickness /cm	Sand/kg	Lime/kg	Gypsum/kg	Diatomite/kg	Mica/kg	Water/kg
Fine sandstone	2.33	17.04	1.42	1.42	0	0	1.99
Coarse sandstone	2.5	19.37	1.21	1.21	0	0	2.18
Siltstone	2.16	15.82	1.19	0.79	0	0	1.78
Sandy mudstone	2	14.82	1.15	0.49	0	0	1.65
B ₄ ² coal seam	1.5	11.01	0.96	0.41	0	0	1.24
B ₄ ¹ coal seam	2	14.68	1.28	0.55	0	0	1.65
B ₃ coal seam	1.8	13.21	1.16	0.50	0	0	1.49
B ₂ coal seam	3	22.02	1.93	0.83	0	0	2.48
Equivalent surrounding rock region.		2.55	0.83	4.12	1.00	0	0.85
Reinforced region		4.99	0.27	2.49	0.5	0	0.83
Cracked region		7.74	0.086	0.43	0	0.43	0.87

Table 3. Monolayer ratio of similar model materials for each rock layer.

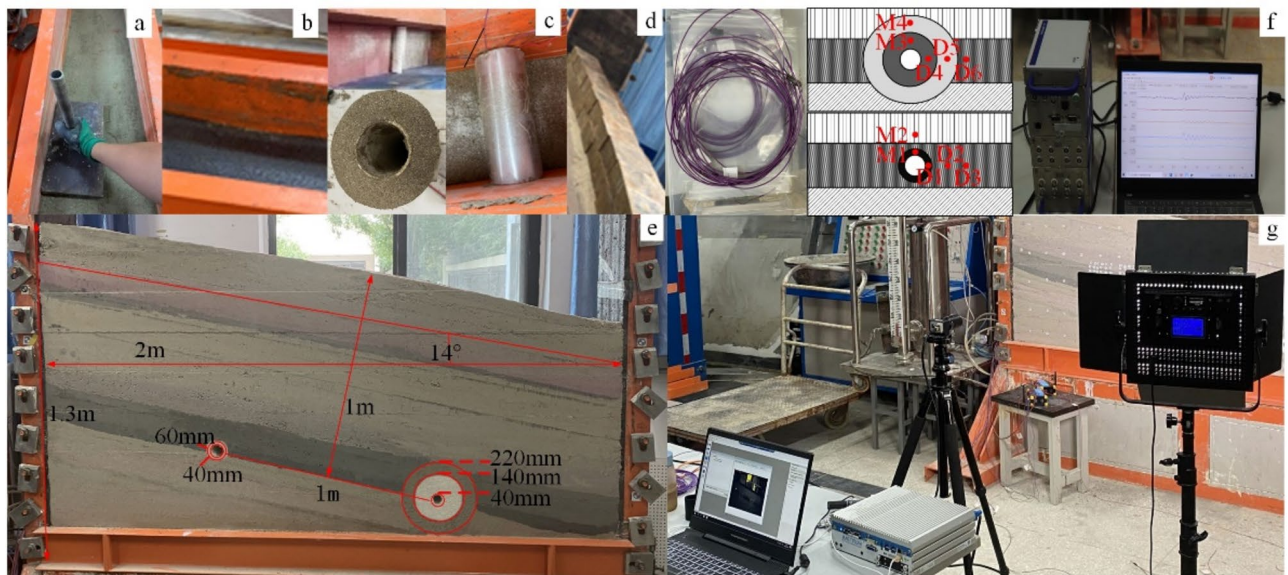


Fig. 5. Physical similarity model.

rock of the unmodified roadway, D1, D2 and D3 at the center and outside of the equivalent surrounding rock, respectively. In-situ modified upper reinforced region and cracked region center position M3, M4, roadway helper reinforced region and cracked region center position and distance from the outside of the cracked region have 50 mm position D4, D5, D6. The sensor monitoring location and monitoring system are shown in Fig. 5f. The digital speckle measurement system is used to monitor the model's displacement during the experiment, as shown in Fig. 5g.

During the experiment, in order to verify the energy absorption, wave dissipation, and stress transfer effects of the numerical simulation method for in-situ modified support of the roadway, a dynamic load similar in size to the numerical simulation was applied, that is, a 0.1 kg steel ball was used to freely drop the dynamic wave from a height of 0.65 m directly above the model. Therefore, the generated impact kinetic energy was about 0.65 J, and the actual energy corresponding to the experiment was about 1×10^8 J.

Numerical simulation

Establishment of models and boundary conditions

PFC, 3DEC, FLAC and ABAQUS are commonly used in rock mass numerical simulation. Among them, PFC has advantages in the study of particle flow meso mechanism, 3DEC in the sliding analysis of block structural plane, and FLAC in the rapid calculation of large deformation. ABAQUS is based on its comprehensive processing ability for the composite problem of “material nonlinearity+geometric nonlinearity+contact nonlinearity”, which exactly fits the complex dynamic characteristics of energy accumulation release redistribution in the evolution process of rockburst. Therefore, ABAQUS numerical simulation software is selected to analyze the support of coal mine roadway under dynamic load impact.

Figure 6 is a numerical calculation model. According to coal's situation and rock strata in the physical similarity model experiment and the above working face, the elastic-plastic deformation model of coal and rock

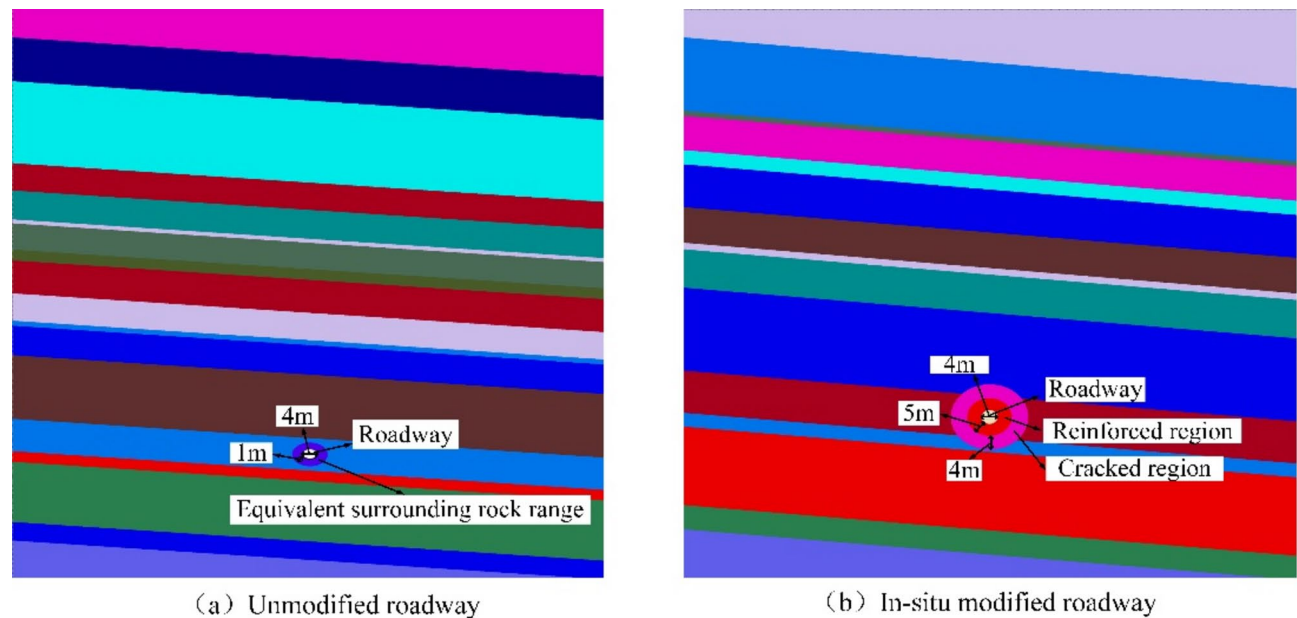


Fig. 6. Numerical calculation model.

Lithology	Density/kg/m ³	Tensile strength/MPa	Modulus of elasticity/GPa	Shear modulus/GPa	Poisson's ratio	Cohesion/MPa	Angle of internal friction/°
Siltstone	2467	2.33	21.26	8.50	0.25	16.22	31.74
Fine sandstone	2688	3.17	34.06	14.07	0.21	21.38	28.86
Coarse sandstone	2543	0.43	2.58	1.09	0.02	2.16	30.00
Sandy mudstone	2546	2.42	11.20	4.41	0.27	5.42	30.41
B ₄ ² coal seam	1388	1.97	2.90	2.01	0.21	3.81	37.49
B ₄ ¹ coal seam	1374	2.02	7.49	2.88	0.25	3.81	37.49
B ₃ coal seam	1356	1.91	2.10	2.03	0.24	3.56	35.00
B ₂ coal seam	1640	2.15	2.50	1.91	0.25	4.70	29.00
B ₁ coal seam	1303	2.02	2.20	1.12	0.23	4.50	31.00
Equivalent surrounding rock region	5000	10.00	100.00	30.00	0.25	40.00	20.00

Table 4. Numerical simulation of material properties of each rock layer.

in the working face is established using ABAQUS numerical simulation software. To reduce the wave springback and reflection disturbance^{47–50}, it is determined that the size of the model is $X \times Y \times Z = 150 \text{ m} \times 2 \text{ m} \times 150 \text{ m}$, the X axis is the coal seam tendency, the Y axis is the coal seam's strike, and the Z axis is the upper and lower boundary height of the model. The distance between the upper surface and the roadway of the model is 100 m, the coal strata are arranged along the dip angle of 14°, and the roadway's diameter is 4 m. The surrounding rock around the unmodified roadway is within 1 m of the equivalent O-shaped shed support, as shown in Fig. 6a. See Table 4 for the rock properties of surrounding rock supported by O-shaped shed. The thicknesses of the cracked region and reinforced region of the in-situ modified roadway are 4 and 5 m, respectively, and the degree of modification is reduced to 10% of the original rock attribute and increased to 90% of the original rock attribute, as shown in Fig. 6b.

The model's mesh is divided into a regular hexahedral structure, and the model's boundary conditions are as follows: the boundary of the model's bottom is fixed, and the normal constraint is adopted before and after. The pressure of the overlying strata on the model is calculated as 6.5 MPa and loaded to the model's upper boundary in the form of stress. Each coal and rock stratum is calculated by the Mohr Coulomb yield criterion. It can be seen from the geological borehole data that the mechanical and physical parameters of different strata in the numerical simulation refer to the indoor physical test data. The reinforced region and the cracked region simulate the corresponding coal and rock mass by raising and decreasing the corresponding percentage material properties, as shown in Table 4.

Dynamic load exertion

According to the characteristics of the ABAQUS numerical simulation software, the simple harmonic P wave is input for simulation, the specific waveform is shown in Formula (1), and the input impulse P wave waveform is shown in Fig. 7.

$$V(t) = \frac{1}{2} V_0 \left[1 - \cos\left(\frac{2\pi t}{\tau}\right) \right] \quad (1)$$

In the formula, V_0 is the shock wave velocity's amplitude, τ is the time span of the shock wave, and t is the shock wave's period. $\tau = 1/f$, where f is the shock wave's frequency.

According to the attenuation trend of microseismic monitoring signals, different rock strata have different damping. After long-distance transmission, the high-frequency shock wave is basically completely dissipated, and the low-frequency shock wave with large energy propagates to the surrounding rock near the roadway. It has a serious impact on roadway that supports facilities and destroys the roadway that surrounds rock and supporting equipment. At the same time, according to the historical microseismic monitoring data of the mine, the microseismic impact frequency is generally 5~20 Hz, so the input harmonic P wave frequency is 20 Hz. According to the above rock burst at the working face, the dynamic shock wave often comes from the roadway roof. This paper only studies the in-situ modified support of roadway surrounding rock under the action of vertical dynamic shock wave, and does not consider the different incident angles of dynamic wave. Therefore, the waveform input direction is vertical downward.

There are more than 1×10^5 J large energy events in the mine. At the same time, to maintain consistency with the physical similar model, 1×10^8 J of energy is input to the model roof for simulation calculation. Consider the formula between the peak velocity and energy of rock particles proposed by A. McGarr et al. (2), as well as the relation formula between the vibration center, impact failure distance r and impact strength (3):

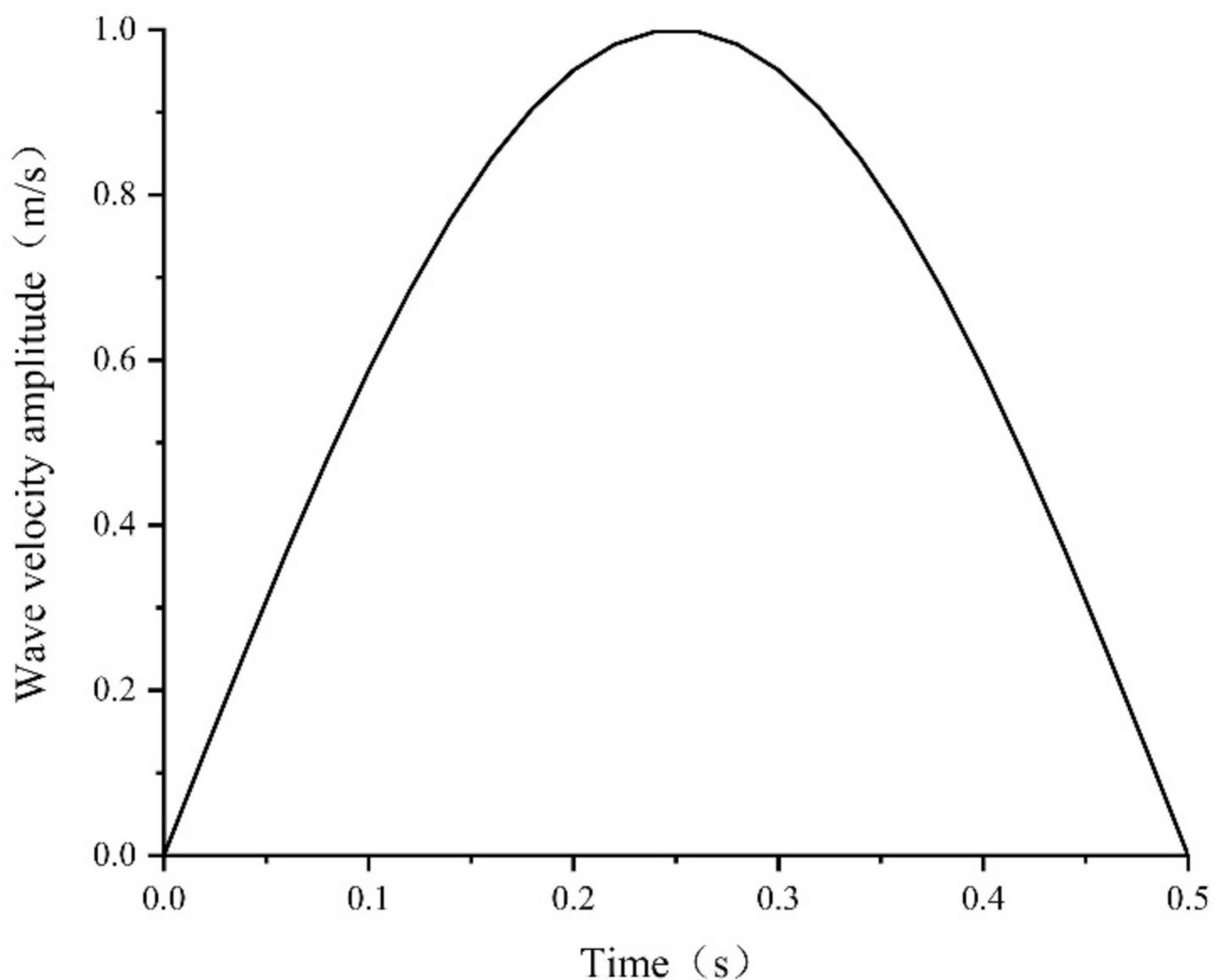


Fig. 7. Impulse P wave waveform.

$$lg\gamma_{rv} = 3.95 + 0.57M_L \quad (2)$$

$$lgE_L = 1.8 + 1.9M_L \quad (3)$$

In the formula, r is the distance between the vibration center and the impact point of the rock, v is the peak velocity of the rock particle, rv is the shock wave's magnitude, and the shock's unit is the same as that of the shock wave energy.

Through the analysis of Formulas (1), (2) and (3), it is found that when the peak particle velocity of the shock P wave is 6.3 m/s and the distance between the roadway and the shock wave source is 100 m, the maximum energy produced by the shock P wave is approximately 1×10^8 J. The model is calculated by global damping, and the typical critical damping ratio is 5%. Through the modal analysis of the numerical model, it is determined that the Rayleigh damping coefficient $\alpha = 1.4191$, while $\beta = 0.0017$. According to the microseismic monitoring data of the mine and previous studies, it is shown that the general duration of microearthquakes is 0.3 ~ 1.5 s, so the simulated dynamic loading time is 0.5 s. The dynamic stress monitoring points in the same position as the similar simulation experiment are arranged in the process of dynamic load loading.

Result analysis

Static stress analysis

As shown in Fig. 8, the comparison chart of the maximum principal stress between the unmodified roadway and the in-situ modified roadway is presented based on the numerical simulation results. From Fig. 8a, it can be seen that under vertical impact dynamic load, the area near the unmodified roadway is a highly concentrated static stress area, distributed on both sides of the roadway, with a maximum of about 30 MPa. From Fig. 8b, it can be seen that after in-situ modification of the surrounding rock of the tunnel, the highly concentrated static stress zone moves away from the periphery of the tunnel and shifts to the outside of the cracked region, with a maximum principal stress of about 27 MPa. The cracked and reinforced regions form an effective stress reduction area, reducing the static stress carried by the roadway itself.

Displacement analysis

As shown in Fig. 9, the comparison between the numerical simulation and similar simulation results of vertical displacement between unmodified and in-situ modified tunnels is presented. From Fig. 9a, it can be seen that under the action of vertical dynamic load, the equivalent surrounding rock region and original rock region of the unmodified roadway have vertical displacements of about 35, 15 mm and 0.30, 0.13 mm respectively in numerical simulation and similar simulation experiments, and the vertical displacements of the top and bottom plates are about 75, 35 mm and 0.40, 0.25 mm respectively. From Fig. 9b, it can be seen that under the action of large impact dynamic waves, the in-situ modified support roadway reinforced region and cracked region surrounding rock have vertical displacements of about 10, 20 mm and 0.08, 0.17 mm respectively in numerical simulation and similar simulation experiments, and the vertical displacements of the top and bottom plates are about 40, 8 mm and 0.20, 0.07 mm respectively. Due to the physical model and actual rock displacement in this paper, The ratio is 1:100, therefore, the results of similar simulation experiments and numerical simulation experiments are relatively consistent. The vertical displacement of the two coal rock masses in the reinforced region of the in-situ modified roadway was reduced by about 3.6 times compared to the degraded surrounding rock region of the unmodified roadway. The vertical displacement of the degraded surrounding rock region in the in-situ modified roadway reinforced and cracked region roof and floor coal rock mass decreased by about 1.9 and 4.0 times, respectively, compared to the unmodified roadway. However, the vertical displacement of the two sides of coal rock mass in the in-situ modified roadway cracked region increased by about 0.3 times compared to the unmodified roadway original rock region.

From this, it can be concluded that the cracked coal rock mass undergoes sliding and contraction deformation within a reasonable range, absorbing part of the impact energy and playing a role in wave damping and shock

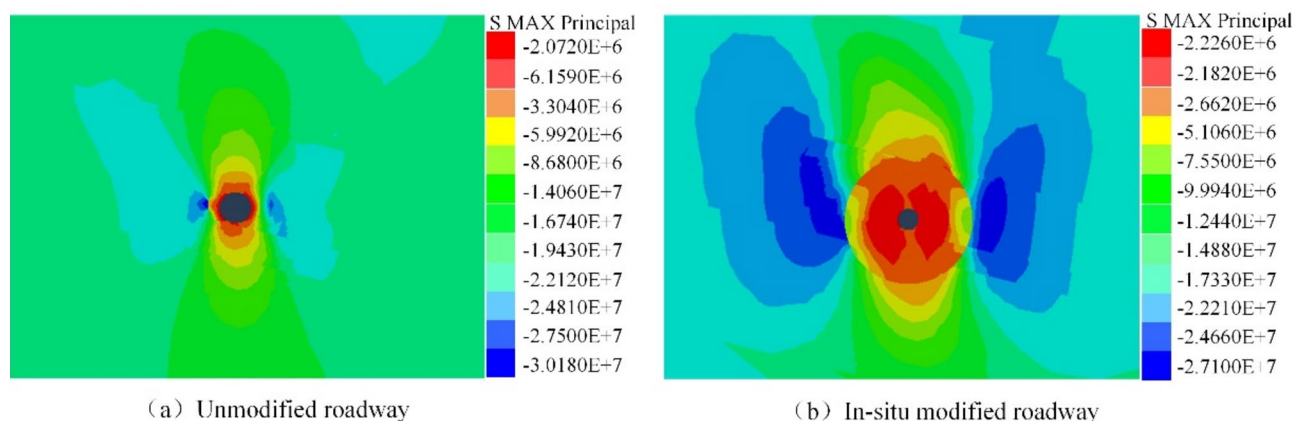


Fig. 8. Cloud map of the maximum principal stress of roadway surrounding rock.

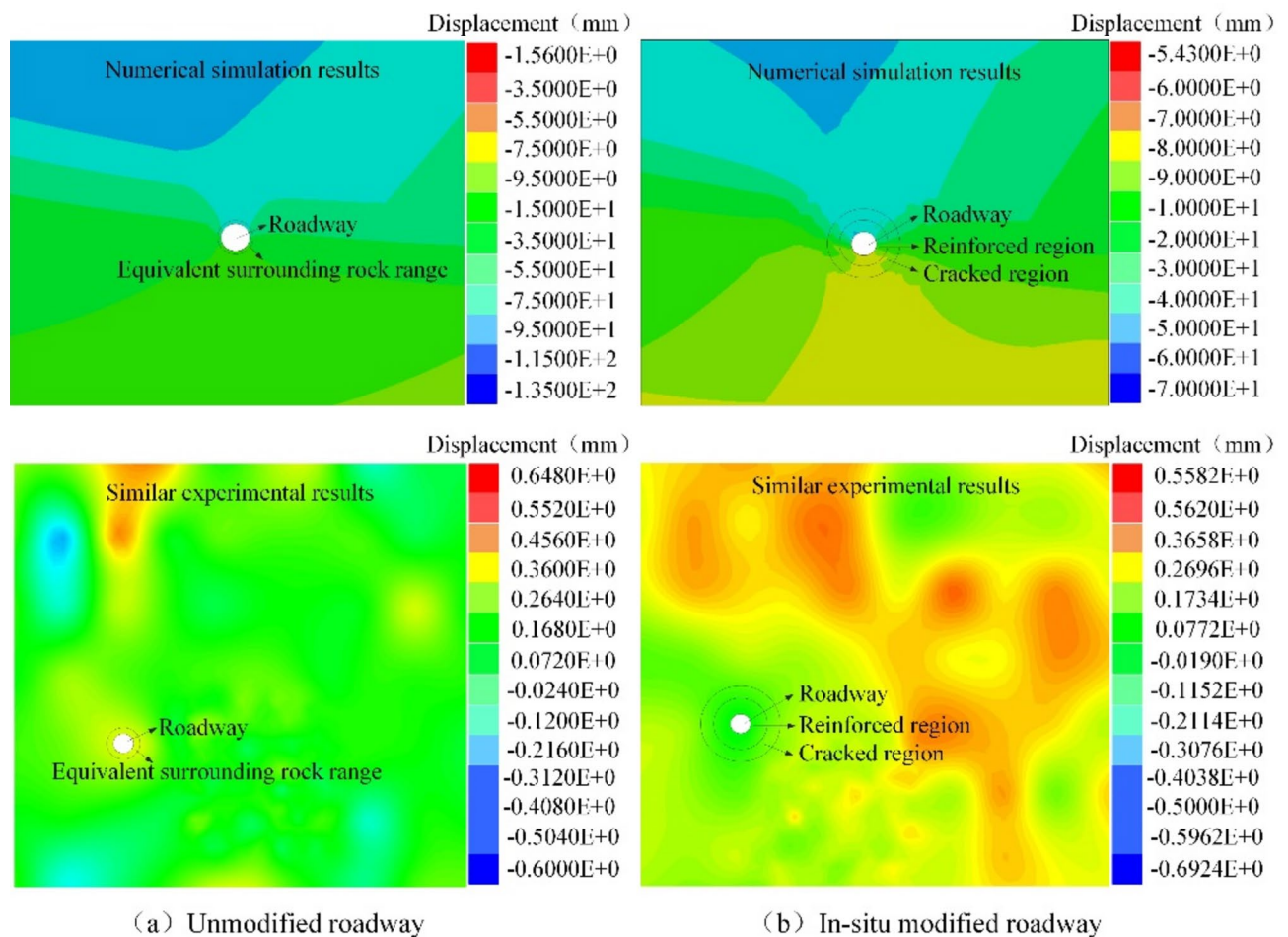


Fig. 9. Cloud map of vertical displacement of roadway surrounding rock.

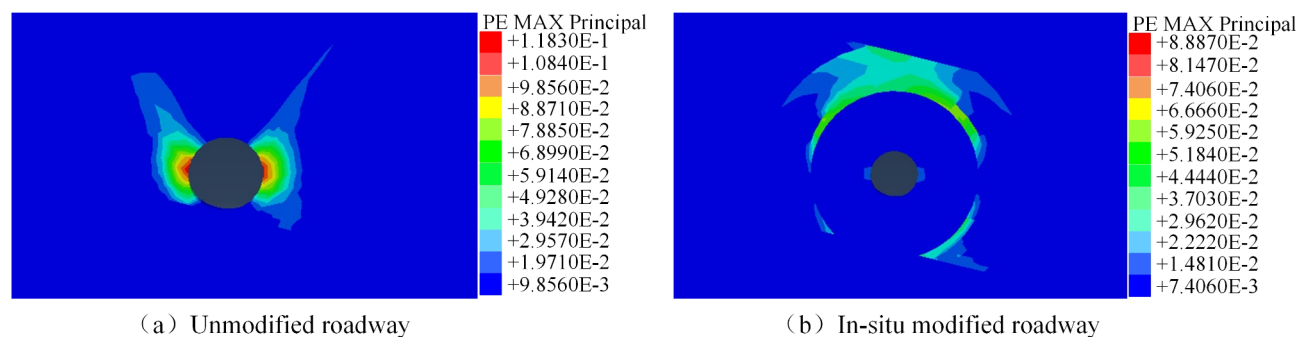


Fig. 10. Cloud map of plastic zone distribution of roadway surrounding rock.

absorption. The surrounding rock of the roadway is subjected to less impact kinetic energy, and at the same time, the ultimate support stress that the coal rock mass reinforced region can withstand increases, resulting in a smaller amount of deformation of the coal rock mass in the reinforced region.

Plastic zone analysis

As shown in Fig. 10, the numerical simulation's plastic zone results of the unmodified roadway and in-situ modified roadway is compared. Figure 10a shows that a large area of plastic damage occurs when the surrounding rock near the unmodified roadway is subjected to large vertical impact dynamic waves. Figure 10b shows that the surrounding rock near the roadway with the in-situ modified support method remains intact and has almost no plastic failure when subjected to a vertical large energy impact dynamic load. Due to the effects of sliding,

friction and deformation of the coal and rock mass in the cracked region, the dynamic stress is consumed and energy is absorbed, and plastic failure occurs only in the cracked region. The surrounding rock mass in the reinforced region has a strong bearing capacity and is affected by less impact dynamic waves to keep the roadway's surrounding rock intact.

Dynamic stress analysis

Figure 11 shows the comparison of numerical simulation results and similar simulation experiments (scaled down by 150 times) of dynamic stress in different positions of the surrounding rock of unmodified and in-situ modified tunnels under vertical impact dynamic load. The two data are in good agreement, indicating that both physical experiments and similar simulations can effectively reproduce the real microseismic process of coal and rock layers.

From Fig. 11a, it can be seen that the peak dynamic stresses of the dynamic waves under impact dynamic load delivered to different measuring points M1, M2, D1, D2, and D3 of the unmodified roadway surrounding rock are approximately 0.41, 0.20, 0.50, 0.40, and 0.90 Mpa, respectively. From Fig. 11b, it can be seen that under the vertical impact of dynamic loads, the maximum dynamic stresses transmitted by dynamic waves to different measuring points M3, M4, D4, D5, and D6 of the surrounding rock in the in-situ modified roadway are approximately 0.14, 0.05, 0.19, 0.10, and 0.70 Mpa, respectively. Comparative analysis shows that the peak dynamic stresses at measurement points M3, M4, D4, D5, and D6 located in the reinforced and cracked regions of the roadway, as well as in the surrounding rock of the roof, have decreased by approximately 2.93, 4.00, 2.63, 4.00, and 1.29 times compared to measurement points M1, M2, D1, D2, and D3 located in the unmodified roadway.

The peak dynamic stress transmitted by the shock wave to measurement points M1 and M3 is greater than that of measurement points M2 and M4, respectively. This is because the elastic modulus of the surrounding

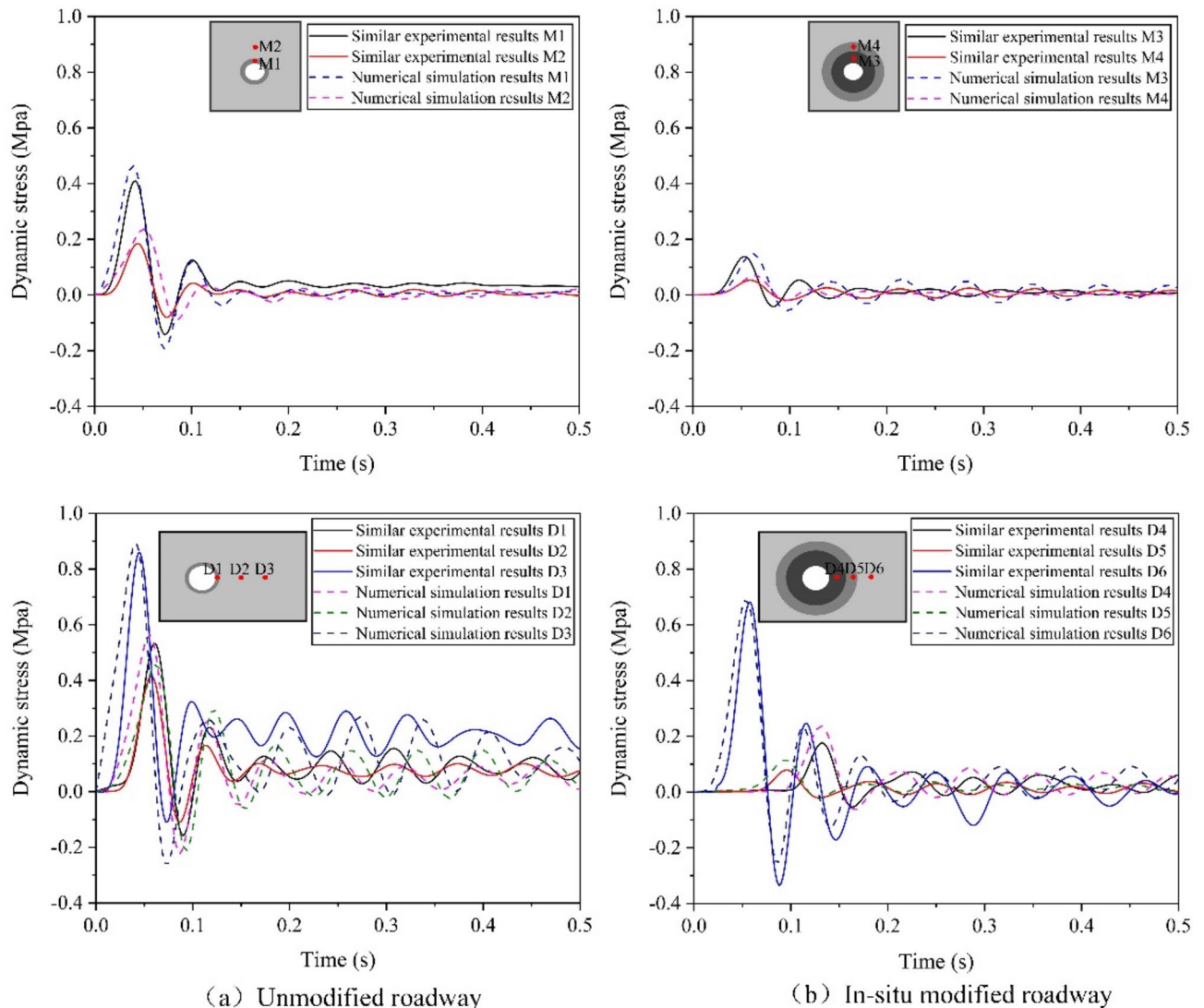


Fig. 11. Dynamic stress curve of roadway surrounding rock.

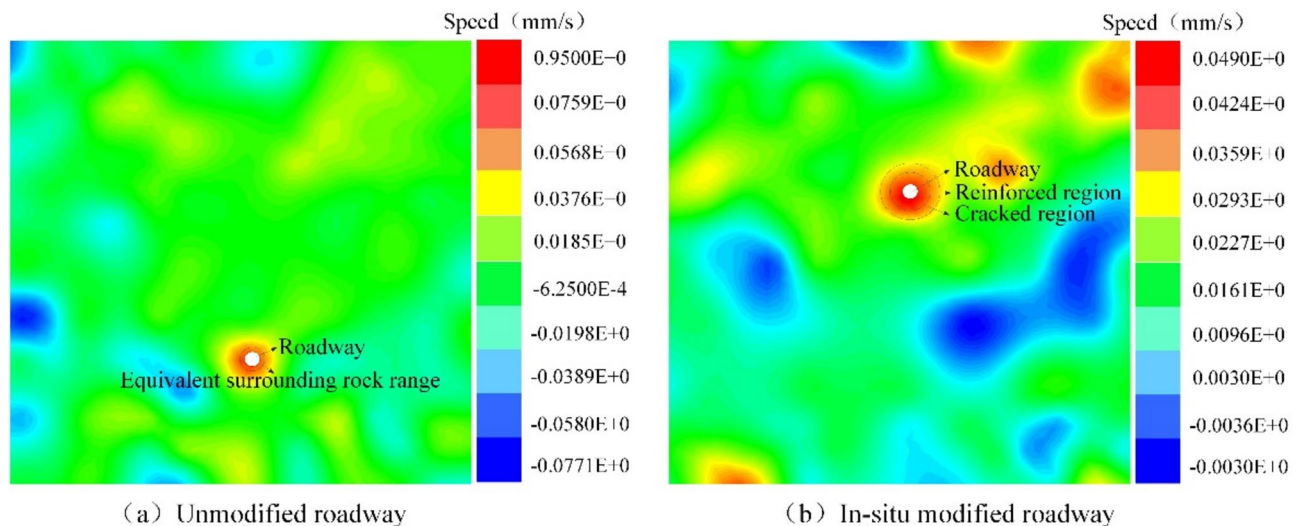


Fig. 12. Cloud map of peak velocity of roadway surrounding rock.

rock and equivalent surrounding rock near the roadway is higher than that of the cracked and reinforced regions. The surrounding rock near the roadway is a reinforced region, which is subjected to a large dynamic stress concentration factor. D2 and D5 are located in the original rock and cracked region, respectively, with a relatively small dynamic stress concentration factor. The peak dynamic stress in the cracked and reinforced regions of the in-situ modified roadway is significantly reduced compared to the unmodified roadway. When the in-situ modified roadway is subjected to a large dynamic load impact, the cracked region of the roadway surrounding rock after in-situ modification has a significant absorption and dissipation effect on the propagation of dynamic waves, ensuring that the roadway is less affected by dynamic loads. The reinforced region of the roadway surrounding rock improves the stability of the roadway itself, and reduces the peak dynamic stress of the surrounding rock near the roadway compared to the degraded surrounding rock region of the unmodified roadway, ensuring the integrity of the roadway surrounding rock and reducing the possibility of impact ground pressure under large impact dynamic loads, protecting the safety of the roadway surrounding rock.

Kinetic energy dissipation analysis

The loss of impact kinetic energy is mainly caused by the reflection and scattering of shock waves by two different types of rock layers, as well as the deformation and contraction of coal and rock masses, and the magnitude of the dynamic wave impact velocity reflects the magnitude of the impact kinetic energy. In order to study the transmission of vertical impact kinetic energy to the vicinity of the roadway, the peak velocity of the shock wave is analyzed for the kinetic energy loss generated by the vertical impact dynamic load in the cracked and reinforced coal and rock mass zones.

Figure 12 shows the peak velocity cloud maps of surrounding rock in unmodified and in-situ modified tunnels under vertical impact kinetic energy. From Fig. 12a, it can be seen that under the action of vertical impact dynamic load, the peak velocity of the impact dynamic wave transmitted to the surrounding rock of the unmodified roadway is about 0.057~0.095 mm/s. From Fig. 12b, it can be seen that when the dynamic wave propagates to the in-situ modified roadway surrounding rock, the maximum velocity of the coal rock mass points in the reinforced and cracked regions is about 0.036~0.049 mm/s. The peak velocities of coal and rock mass points in the reinforced and cracked regions of the in-situ modified roadway decreased by about 37% and 48% respectively compared to the unmodified roadway. From the perspective of rock burst prevention mechanism, the coal and rock mass in the cracked region can effectively dissipate the energy of shock dynamic stress wave and significantly reduce the dynamic stress peak transmitted to the reinforced region by forming multiple reflection interfaces and wave impedance difference layers. At the same time, by improving the structural integrity and mechanical parameters of surrounding rock in the grouting reinforced region, the surrounding rock bearing system has a significant dynamic load strengthening effect, and its dynamic bearing capacity has been significantly improved, which can effectively resist the destructive effect of residual dynamic stress. This coordinated prevention and control mechanism of "energy consumption in cracked region and bearing in reinforced region" realizes the consumption and control of dynamic stress through the systematic effect of hierarchical energy dissipation and cascade bearing.

When impact ground pressure occurs, the ejection speed of surrounding rock particles in the tunnel is faster and the ejection kinetic energy is greater. It can be seen that the in-situ modified coal rock mass can reduce the propagation speed of shock waves and greatly dissipate the impact kinetic energy of vertical impact dynamic loads propagating in the coal rock mass.

Based on the above analysis, it can be concluded that the in-situ modified support method for roadway surrounding rock is relatively reliable. The high static stress borne by the in-situ modified roadway surrounding rock is transferred to the outside of the cracked region, and the arch bridge effect is greatly reduced, effectively

reducing the transmission of shock dynamic waves and greatly consuming the impact kinetic energy. It effectively controls the displacement of the roadway surrounding rock, maintains the stability and integrity of the roadway, ensures the safety of the roadway surrounding rock under large impact dynamic loads, and can effectively prevent the occurrence of impact ground pressure. Compared with traditional support methods such as O-shaped sheds and U-shaped steel, the improved in-situ modified support method proposed in this paper can not only improve the stability of tunnel surrounding rock, shorten the support period of tunnel surrounding rock, but also effectively reduce the cost of tunnel surrounding rock support.

Conclusion

This article studies the reliability of in-situ modified support methods for roadway surrounding rock under vertical impact loads through numerical simulations and physical model experiments, that is, the support capacity of roadway surrounding rock after crushing and reinforced treatment. The numerical simulation and physical model experimental results have high consistency, indicating that this support method can effectively protect the integrity of the surrounding rock of the roadway. A comparative analysis was conducted on the static stress redistribution, displacement, plastic zone distribution, dynamic stress response, and kinetic energy dissipation characteristics of the surrounding rock of the original rock roadway and the in-situ modified roadway under the same impact load. The specific conclusion is as follows:

- (1) The reinforced region effectively increases the stress bearing limit of the surrounding rock, and the cracked region and the reinforced region form an effective stress reduction zone, transferring the highly concentrated static stress area to the outside of the cracked region. The static stress carried by the roadway itself is reduced, ensuring the integrity of the roadway surrounding rock.
- (2) The surrounding rock in the reinforced region effectively controls the displacement of the roadway roof, floor and slope, the plastic loss in this area is reduced, the surrounding rock in the cracked region has a reasonable range of extrusion deformation, and the plastic damage of the surrounding rock in the cracked region is increased.
- (3) Under the vertical impact dynamic load of the roof, the peak dynamic stress on the roadway support and roof surrounding rock decreases, and the maximum dynamic stress is located on the outer side of the cracked region, reducing the impact velocity of the roadway surrounding rock and effectively absorbing and consuming kinetic energy. The reinforced region and cracked region surrounding rock jointly protect the safety of production operations in the roadway.

Data availability

The original contributions presented in the study are included in the article.

Received: 21 January 2025; Accepted: 10 April 2025

Published online: 07 May 2025

References

1. Qiang, W. et al. Discussion on the main problems and countermeasures for Building an upgrade version of main energy (Coal) industry in China. *J. China Coal Soc.* **44** (6), 1625–1636 (2019).
2. Zhang, W. et al. Mechanism of rock burst revealed by numerical simulation and energy calculation. *Shock Vib.* **1** (2020), 1–15 (2020).
3. Tian, X. Y. et al. Risk assessment and mechanism of rock burst for deep soft coal roadways. *Sci. Rep.* **15** (1), 7054–7054 (2025).
4. Qiu, P. Q. et al. Mitigating rock burst hazard in deep coal mines insight from dredging concentrated stress: A case Study - ScienceDirect. *Tunn. Undergr. Space Technol.* **115**, 104060 (2021).
5. Han, J. et al. A coal burst model based on roof vibration and coal slippage. *IOP Conf. Series: Earth Environ. Sci.* **570.4** (9), 042–037 (2020).
6. Chen, F. et al. Study on the size effect of rock burst tendency of red sandstone under uniaxial compression. *Sci. Rep.* **14** (1), 16402 (2024).
7. Xlab, C. & Yc., B. Determination of pillar width to improve mining safety in a deep Burst-prone coal Mine–Science direct. *Saf. Sci.* **113**, 244–256 (2019).
8. Wang, Z. et al. Analysis and optimizations on retreating mining measures of rock burst prevention on steeply dipping Thick coal seam in deep exploitation. *Procedia Eng.* **26**, 1 (2011).
9. Obert, L. & Duvall, W. I. *Rock Mechanics and Design of Structures in Rock* pp. 650–654 (John Wiley & Sons, 1967).
10. Blake, W. & Hedley, D. G. F. Case Studies from North American Hard-Rock Mines, Society for Mining Metallurgy and exploration, pp. 515–518 (2003).
11. Ma, N. J. et al. Occurrence mechanisms and judging criterion on circular tunnel butterfly rock burst in homogeneous medium. *J. China Coal Soc.* **41** (11), 2679–2688 (2016).
12. Kang, H. et al. Study on small borehole pre-tensioned cable reinforcing complicated roadway. *Chin. J. Rock Mechan. Eng.* **22** (3), 387–390 (2003).
13. Kang, H. P. Study and application of complete rock bolting technology to coal roadway. *Chin. J. Rock Mechan. Eng.* **24**, 161–166 (2005).
14. Kang, H. P. et al. Analysis on stability of rock surrounding heading faces and technical approaches for rapid heading. *J. China Coal Soc.* **46**, 07 (2021).
15. Kang, H. P. et al. Roadway strata control technology by means of Bolting-modification-destressing in synergy in 1 000 m deep coal mines. *J. China Coal Soc.* **45**, 845–864 (2020).
16. Kang, H. P. et al. Strata control technology and applications of Non-pillar coal mining. *J. China Coal Soc.* **47**, 16–44 (2022).
17. He, M. et al. (ed, C.) Mechanics characteristics and applications of prevention and control rock bursts of the negative Poisson's ratio effect anchor. *J. China Coal Soc.* **39** 2 214–221 (2014).
18. He, M. C. et al. Mechanical characteristics and engineering applications of bolt/cable with negative poisson's Ratio¹. *Mech. Eng.* **44**, 75–87 (2022).
19. He, M. C. & Guo, Z. B. Mechanical property and engineering application of anchor bolt with constant resistance and large deformation. *Chin. J. Rock Mechan. Eng.* **33**, 214–221 (2014).

20. Qi, Q. X. et al. Preliminary theoretical study on stress flow thought for coal bump and its control. *Chin. J. Rock Mechan. Eng.* **38**, 05 (2021).
21. Qi, Q. X. et al. Theory and technical framework of prevention and control with different sources in Multi-scales for coal and rock dynamic disasters in deep mining of coal mines. *J. China Coal Soc.* **43**, 1801–1810 (2018).
22. Pan, Y. S. et al. Desing Ofanti-scour support based on theory of Pendulum-type wave. *Chin. J. Rock Mechan. Eng.* **32**, 1537–1543 (2013).
23. Pan, Y. S. et al. Theory and technology of three levels support in Bump-prone roadway. *J. China Coal Soc.* **45**, 1585–1594 (2020).
24. Lu, X. F. & Pan, Y. S. Stress wave propagation and decay law and test Analtsis of surrounding rock by Rigid-Flexible coupling support. *Eng. Mech.* **30**, 345–349 (2013).
25. Lu, X. F. et al. Law of roadway deformation of energy absorbing support under explosive loading. *Chin. J. Geotech. Eng.* **33**, 1222–1226 (2011).
26. Huang, Z. W. et al. Application of impact-constant resistance anchor support theory in rock burst mine. *J. China Coal Soc.* **41**(S1), 21–28 (2016).
27. Jiao, J. K. et al. Burst failure mechanism of roadway anchorage bearing structure under dynamic load disturbance. *J. China Coal Soc.* **46**(S1), 94–105 (2021).
28. Anders, A. Laboratory testing of a new type of energy absorbing rock Bok. *Tunn. Undergr. Space Technol.* **20** (4), 291–300 (2005).
29. Anders, A. Dynamic testing of steel for a new type of energy absorbing rock bolt. *J. Constr. Steel Res.* **62** (5), 501–512 (2006).
30. Gaudreau, D. et al. Apparatus and method for a yieldable tendon mine support. *US Patent*. **6**, 390 (2002).
31. D, R. G. *Methodology for the design of dynamic rock supports in burst prone ground* (McGill University, 2013).
32. Li, C. C. *DOUCET, C., Performance of D-bolts Under Dynamic Loading Conditions* 45pp. 192–204 (Rock Mechanics and Rock Engineering, 2012).
33. Li, C. C. A new Energy-absorbing bolt for rock support in high stress rock masses. *Int. J. Roc Mech. Min. Sci.* **47**, 396–404 (2010).
34. Zhang, Q. et al. Assessment of rockburst risk in deep Nining: An improved comprehensive index method. *Nat. Resour. Res.* **30**, 1817–1834 (2021).
35. Wang, J. et al. Mechanism of rock burst occurrence in specially Thick coal seam with rock parting. *Rock Mech. Rock Eng.* **49** (5), 1953–1965 (2016).
36. Jiang, L. et al. *Dynamic Analysis of the Rock Burst Potential of A Longwall Panel Intersecting with A Aault* pp. 1–18 (Rock Mechanics and Rock Engineering, 2019).
37. Li, N. & Jimenez, R. A logistic regression classifier for Long-term probabilistic prediction of rock burst hazard. *Nat. Hazards*. **90** (1), 197–215 (2018).
38. Rong, H. et al. A method for assessing the risk of rockburst based on coal-rock mechanical properties and In-Situ ground stress. *Sci. Rep.* **14** (1), 26073–26073 (2024).
39. Tan, G. H. et al. Influence of bedding angle on rockburst behavior of sandstone: insights from energy storage and dissipation. *Bull. Eng. Geol. Environ.* **84** (3), 156–156 (2025).
40. Wang, C. et al. *Performance study of a novel j energy-absorbing bolt under controlled dynamic loads* 1–20 (Rock Mechanics and Rock Engineering, 2025). prepublsh.
41. Kaiser, P. K. & Cai, M. Design of rock support system under rockburst condition. *J. Rock Mech. Geotech. Eng.* **4** (3), 215–227 (2012).
42. Gao, M. et al. Strong-soft-strong mechanical model for controlling roadway surrounding rock subjected to rock burst and its application. *Rock. Soil. Mech.* **29** (2), 359–364 (2008).
43. Gao, M. et al. A new theoretical model of rock burst-prone roadway support and its application, *Geofluids*, 5549875. (2021).
44. Wang, G. F. et al. Applicability of Energy-absorbing support system for rockburst prevention in underground roadways. *Int. J. Rock Mech. Min. Sci.* **132**, 104396 (2020).
45. Chi, P., Ren, D. H. & Wei, S. J. Design of roadway support for soft coal seam back mining in Wangxingzhuang coal mine. *Int. J. Energy*. **5** (2), 10–13 (2024).
46. Bin, T. et al. *Strength of fabricated enclosed roadway support structure for TBM-excavated coal mine roadways: Experimental and numerical study* 131 (Tunnelling and Underground Space Technology incorporating Trenchless Technology Research, 2023).
47. Zhao, M. et al. Time-domain stability of artificial boundary condition coupled with finite element for dynamic and wave problems in unbounded media. *Int. J. Comput. Methods*. **16** (04), 1850099 (2019).
48. Yi, H. et al. *Influence of long-term dynamic load induced by high-speed trains on the accumulative deformation of shallow buried tunnel linings* 84pp. 166–176 (Tunnelling and Underground Space Technology, 2019).
49. Su, W. et al. A scheme for switching boundary condition types in the integral Static-dynamic analysis of Soil-structures in Abaqus. *Soil Dyn. Earthq. Eng.* **141**, 106458 (2021).
50. Gu, Q. Y. et al. Application of long-distance drilling and blasting technology to prevent rock bursts in high-level roofs. *Appl. Sci.* **15** (4), 1821–1821 (2025).

Acknowledgements

Authors acknowledge support from Beijing City Postdoctoral Fund (2024-ZZ-74); Beijing Association for Science and Technology 2024–2026 Young Talents Promotion Project; Henan Province Science and Technology Research Project (2421023200072, 242102321011); Henan Province Housing and Urban-Rural Construction Science and Technology Plan Project (K-2318); Anhui Province Postdoctoral Research Projects, China (2024C972).

Author contributions

H.Z. participated in the whole process of work; Y.L., T.L., H.Y., J.L., Y.Q., Y.L., and Y.D. revised and checked this paper; S.L., Y.C., F.L., and S.G. provided technical guidance and experimental support. All authors have read and agreed to the published version of the manuscript.

Declarations

Competing interest

The authors declare no competing interests.

Additional information

Correspondence and requests for materials should be addressed to H.Z., T.L. or Y.L.

Reprints and permissions information is available at www.nature.com/reprints.

Publisher's note Springer Nature remains neutral with regard to jurisdictional claims in published maps and institutional affiliations.

Open Access This article is licensed under a Creative Commons Attribution-NonCommercial-NoDerivatives 4.0 International License, which permits any non-commercial use, sharing, distribution and reproduction in any medium or format, as long as you give appropriate credit to the original author(s) and the source, provide a link to the Creative Commons licence, and indicate if you modified the licensed material. You do not have permission under this licence to share adapted material derived from this article or parts of it. The images or other third party material in this article are included in the article's Creative Commons licence, unless indicated otherwise in a credit line to the material. If material is not included in the article's Creative Commons licence and your intended use is not permitted by statutory regulation or exceeds the permitted use, you will need to obtain permission directly from the copyright holder. To view a copy of this licence, visit <http://creativecommons.org/licenses/by-nc-nd/4.0/>.

© The Author(s) 2025